



ChemComm

**Synthesis and photochemical properties of caged peroxides
for photocontrol of cellular oxidative stress**

Journal:	<i>ChemComm</i>
Manuscript ID	CC-COM-03-2023-001192.R1
Article Type:	Communication

SCHOLARONE™
Manuscripts

COMMUNICATION

Synthesis and photochemical properties of caged peroxides for photocontrol of cellular oxidative stress†

Received 00th January 20xx,
Accepted 00th January 20xx

Mieko Tsuji*^a, Haruno Taira^a, Taro Udagawa^b, Tatsuya Aoki^a, Tasuku Hirayama^a and Hideko Nagasawa*^a

DOI: 10.1039/x0xx00000x

We developed a caged hydroperoxide, BhcTBHP, releasing prooxidant TBHP under blue light irradiation. MitoTBHP with triphenylphosphonium at the position 7 triggered selective oxidative stress and membrane depolarization in mitochondria upon photoirradiation. This study presents a powerful tool for studying redox signaling and oxidative stress in living cells.

Reactive oxygen species (ROS) may cause cell damage and have been linked to a variety of human diseases, including cancer, heart diseases and neurodegenerative diseases. In addition, numerous investigations during the last two decades have demonstrated that ROS also plays a pivotal role in regulating various aspects of normal physiological cell function^{1,2}. ROS induce a range of oxidative post-translational modifications depending on their type and local concentration^{1,2}, which are referred to as redox signalling at physiological levels or oxidative stress at elevated levels. Redox signalling is mainly mediated by the oxidative modification of cellular cysteines by H₂O₂.³ The production and reaction of ROS in cells is spatially and temporally constrained.⁴ Exogenous oxidative stress inducers like H₂O₂ and *tert*-butyl hydroperoxide (TBHP) have conventionally been used to study the roles of ROS in cells.^{5–8} TBHP is more thermodynamically stable than H₂O₂ and is commonly used as a popular alternative to H₂O₂.⁹ In general, these oxidative stress inducers operate non-specifically on the whole cell, making compartmentalisation and spatiotemporal regulation of ROS production and responses problematic. The recent development of new ROS detection and redox probes has enabled the detection of ROS formation in various cellular

compartments of living cells.^{4,10,11} Furthermore, photo-cleavable caged compounds, which may release a range of effector molecules in a spatiotemporally regulated manner upon light irradiation, have emerged as powerful tools for the targeted perturbation of biological processes. However, most caged compounds that can be used to study oxidative stress and redox signalling are limited to photodonors that emit reactive nitrogen oxide species.¹² Functional molecules for light-induced ROS generation include photosensitizers that generate singlet oxygen (¹O₂) and superoxide,¹³ and caged hydroquinone, which reduces oxygen molecules to hydrogen peroxide.¹⁴ In contrast, a caged compound that directly releases ROS would be useful for spatiotemporal control of precise oxidative modification in cells.

This paper details the synthesis, properties, and functions of novel caged hydroperoxides (BhcTBHP) that release the prooxidant TBHP upon photoirradiation. We also developed membrane-permeable and mitochondria-targeted derivatives (AcBhcTBHP and MitoTBHP) capable of inducing oxidative stress in cells (See Fig. 1). Furthermore, in the presence of MitoTBHP, the mitochondrial membrane potential (MMP) was successfully depolarised upon light irradiation, demonstrating that ROS signalling may be induced in mitochondria at the appropriate time in living cells.

Fig. 1 depicts the structure of the novel caged hydroperoxides developed in this study as well as the mechanism of the photo-uncaging reaction. We chose TBHP as a caged effector molecule because it is relatively stable and widely used as an oxidative stress inducer as described above. Moreover, the 6-Bromo-7-hydroxycoumarin-4-ylmethyl (Bhc) group^{15,16} was selected as the photoremovable protecting (caging) group because of its higher photosensitivity than the nitrobenzyl-based photolabile groups. Heterolytic bond cleavage or competition between homolytic and heterolytic cleavage has been proposed as a mechanism for photocleavage of coumarin derivatives.¹⁷ Although the possibility of homolytic cleavage cannot be entirely excluded, previous studies¹⁷ have

^aLaboratory of Pharmaceutical and Medicinal Chemistry, Gifu Pharmaceutical University, 1-25-4 Daigaku-nishi, Gifu, 501-1196, Japan.
e-mail: tsuji@gifu-pu.ac.jp, hnagasawa@gifu-pu.ac.jp

^bDepartment of Chemistry and Biomolecular Science, Faculty of Engineering, Gifu University, 1-1 Yanagido, Gifu 501-1193, Japan

†Electronic Supplementary Information (ESI) available: Full experimental procedures and analysis. See DOI: 10.1039/x0xx00000x

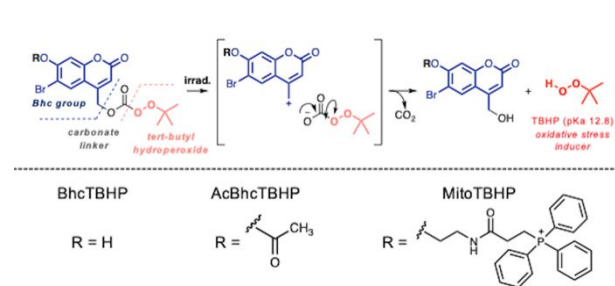


Fig. 1 Strategy of caged TBHP compounds.

provided evidence in support of a heterolytic cleavage mechanism in which a photo $\text{S}_{\text{N}}1$ reaction (solvent-assisted photo-heterolysis) forms ion pairs as intermediates to produce 4-(hydroxymethyl)coumarin.^{18,19} In these reactions, the higher the leaving ability (lower pKa value), the higher is the photochemical quantum yield²⁰. We expected that the photocleavage reaction would not proceed if TBHP was directly bound to the Bhc group because of its low leaving ability and the high pKa value (=12.8). In such cases, coumarin-4-ylmethyl carbonate scaffold should be an alternative photoremovable protecting group for efficient photo-triggered release of alcohols via spontaneous decarboxylation due to the considerably lower pKa (6.4) than that of alcohols.²¹ In this context, the Bhc group and TBHP were linked via a carbonate linker. Based on this BhcTBHP, AcBhcTBHP with 7-O-acetyl group was also synthesized to improve membrane permeability. Furthermore, since Furuta et al. reported²² that alkylation of the 7-hydroxyl group of the Bhc group did not impair the overall photosensitivity, we predicted that an organelle-targeting moiety could be introduced at position 7 and synthesized MitoTBHP with a triphenylphosphonium (TPP) group to target mitochondria²³ (Scheme S1 and S2).

First, the photocleavage of BhcTBHP was evaluated using LC-MS (Fig. 2a). The reaction was conducted using light irradiation at 375 nm (2.5 mW/cm²) under physiological conditions (100 mM phosphate buffer at pH 7.4, 1% DMF). When the solution of BhcTBHP (100 μM) was irradiated for 1 min, the peak of BhcTBHP disappeared, and the peak of photoproduct 1 with the expected m/z 270 appeared at $R_t = 13.8$ min. Next, we evaluated the release of TBHP after irradiation using NBzF, a fluorescent probe for H₂O₂ detection that also modestly responds to TBHP to produce 5-carboxyfluorescein²⁴ (Fig. 2b). A significant increase in fluorescence was observed in the solution of irradiated BhcTBHP at 375 nm (247 $\mu\text{W}/\text{cm}^2$), with a fluorescence intensity as high as 5-fold after 5 min of irradiation (Fig. 2b and 2c). The amount of TBHP was determined from the calibration curve (Fig. S1), which showed that BhcTBHP was efficiently photolyzed to produce quantitative TBHP under physiological conditions.

Regarding the photolysis mechanism, we also considered the possibility that the bromocoumarin moiety undergoes an oxygen-dependent photosensitization reaction via an intersystem crossing from the excited singlet state to the triplet state.²⁵ There are Type I and Type II mechanisms for the generation of ROS by photosensitization reactions. In the Type I mechanism, electron transfer to molecular oxygen from the

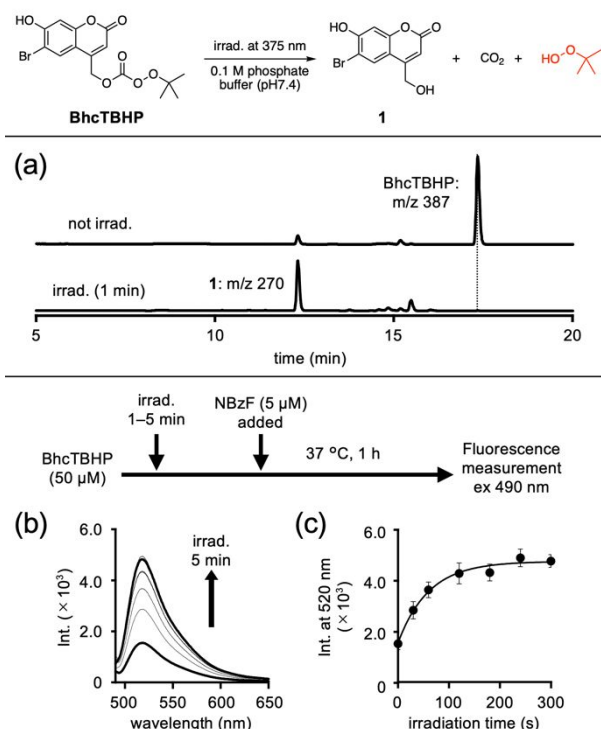
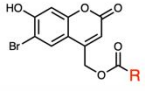


Fig. 2 (a) LC-MS analysis of the reaction of BhcTBHP irradiated at 375 nm (2.5 mW/cm²). (b) Fluorescence response of the reaction between NBzF and irradiated (0.25 mW/cm²) BhcTBHP. (c) Irradiated time course of TBHP releasing from BhcTBHP. Error bars denote standard error (SE; $n \geq 7$).

triplet state produces free radical ROS and H₂O₂. In Type II, on the other hand, ¹O₂ was formed by energy transfer.²⁶ Therefore, we performed fluorescence measurements using NBzF on BhcO^tBu containing *t*-BuOH as an effector instead of TBHP and found no significant fluorescence with or without light irradiation (Fig. S2a), i.e., H₂O₂ was not formed. In addition, no ¹O₂ was generated from the photoirradiated BhcTBHP solution (Fig. S2b). These data suggest that ROS generation via the photosensitization reaction of Bhc derivatives is almost negligible.

Next, photochemical properties of BhcOAc¹⁵ containing acetic acid, and BhcO^tBu were compared with those of BhcTBHP and MitoTBHP (Fig. 3a and S3a). Notably, the photolysis quantum yields of BhcTBHP and MitoTBHP were considerably higher than others. BhcTBHP has an order of magnitude larger uncage cross section ($\epsilon\Phi$), even though the pKa of the leaving group is comparable. On the other hand, MitoTBHP had a reduced $\epsilon(365)$ due to the modification of the hydroxyl group. Thus, the reaction rates of BhcTBHP and MitoTBHP at 365 nm (5 mW/cm²) irradiation were 0.147 s⁻¹ and 0.021 s⁻¹, respectively (Fig. S3b). To investigate the reason for the higher photolysis yield of BhcTBHP than BhcO^tBu, their low-lying excited states were calculated using time-dependent density functional theory (TDDFT). The first excitation was the highest occupied molecular orbital (HOMO)–lowest unoccupied molecular orbital (LUMO) transition (99%). The vertical emission energy of the S1 state of BhcTBHP is 2.55 eV (485 nm), which is comparable to experimental results for Bhc-caged compounds (474 nm)¹⁵ (Table S1). Fig. 3 depicts the optimised geometries and the LUMO of BhcTBHP (left) and BhcO^tBu (right). In BhcTBHP, the

(a)



BhcOAc: R = CH₃
BhcO^tBu: R = OC(CH₃)₃

comp.	λ_{\max}^a (nm)	ϵ (M ⁻¹ cm ⁻¹) ^b	Φ_{365}	$\epsilon\Phi_{365}$ (M ⁻¹ cm ⁻¹)
BhcOAc ^c	373	16,300	0.040 ± 0.003 ^c	652
BhcO ^t Bu	372	14,600	0.037 ± 0.002 ^c	540
BhcTBHP	373	18,500	0.127 ± 0.009 ^c	2.4 × 10 ³
MitoTBHP	330	2,000	0.156 ^d	312

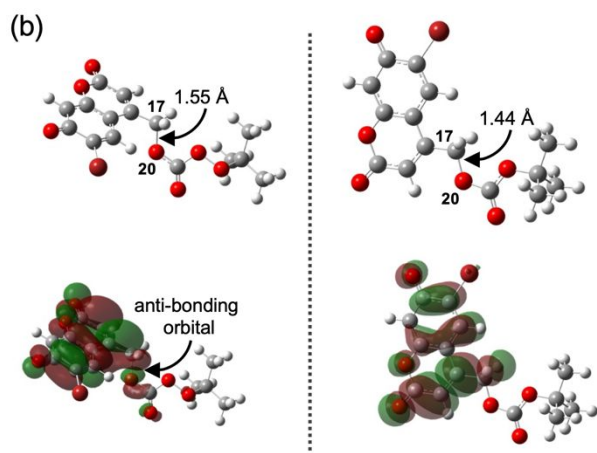


Fig. 3 (a) Photochemical properties. They were measured in 100 mM KCl–10 mM KMops buffer (pH 7.2). ^aMaximum absorption wavelength. ^bMolar extinction coefficient at 365 nm. ^cQuantum yield of disappearance of starting materials. Mean ± SD (^cn=3, ^dn=1). ^eReported values: λ_{\max} 370 nm, $\epsilon(365) = 14,800 \text{ M}^{-1}\text{cm}^{-1}$, $\Phi_{\text{dis}} = 0.037$, $\epsilon\Phi_{365} = 548.19$. (b) Optimized geometries on S1 state and LUMO of BhcTBHP (left) and BhcO^tBu (right) calculated at the TD-B3LYP/6-31G(d) level.

dihedral angle between the C α –O bond and the coumarin plane is 76°, suggesting that the stereoelectronic orbital overlap effect between the σ^* of the CO bond and the π of coumarin stabilizes the transition state and facilitates cleavage of benzylic C–O bond in the photo SN1 reaction.²⁷ In BhcO^tBu, on the other hand, such stereoelectronic effects are not possible because the C α –O bond and the coumarin ring are coplanar. The high photoreactivity of BhcTBHP is also supported by the fact that the CO bond is longer and antibonding.

To confirm the utility of BhcTBHP, we investigated the light-induced release of TBHP in cells using AcBhcTBHP, which permeates the cell membrane and is hydrolysed to BhcTBHP by intracellular esterases. The optimal concentration and treatment time were determined by MTT assays, and stability tests against glutathione (GSH) were performed by HPLC analysis. MCF-7 (RCB1904 by RIKEN BRC) cells were treated with various concentrations of caged compounds for 15 min, cultured for 15 min under UV irradiation or non-irradiation, and subjected to MTT assay. The results showed that AcBhcTBHP was not significantly toxic with or without light irradiation at concentrations up to 100 μM (Fig. S4). Next, to evaluate the stability of BhcTBHP to GSH, it was incubated in the presence of 1 mM GSH at 37 °C for up to 60 min, and the residual amount was measured by HPLC and was found to decrease to 40% after 30 min and to 20% after 60 min (Fig. S5). After 60 min of incubation in the absence of GSH, more than 70% of BhcTBHP

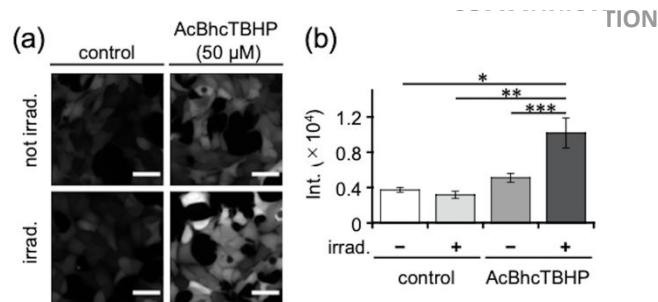


Fig. 4 (a) Confocal fluorescence microscopic images of irradiated MCF-7 cells treated with AcBhcTBHP using NBzFDA. Images were taken at Ex 470 nm and Em range 516–556 nm. Scale bar = 50 μm . (b) Average cellular fluorescence intensity of the MCF-7 cells as determined using Image J. Error bars denote standard error (SE; n=5). * $p < 0.0005$, ** $p < 0.001$, *** $p < 0.01$. Tukey's test.

remained (data not shown). As a result, after MCF-7 cells were treated with AcBhcTBHP (50 μM) for 15 min and irradiated at 375 nm (12 mW/cm²) for 5 min, TBHP released in the cells was detected using NBzFDA (diacetylated NBzF).²⁴ The fluorescence intensity increased dramatically after treatment with AcBhcTBHP and light irradiation, indicating that TBHP was released in the cells. According to Fig. 4, there was actually weak fluorescence in the control and non-irradiated panels. To examine the phototoxicity of blue light, LDH assays were performed after 15 min of exposure to 375 nm (12 mW/cm², 30 mW/cm²) light, but no difference was observed in non-irradiated cells (Fig. S6).

MitoTBHP was also not cytotoxic, and its stability toward GSH was slightly lower than that of BhcTBHP. (Fig. S4 and S5, respectively). It was also observed that MitoTBHP released TBHP intracellularly upon light irradiation (Fig. S7). It is known that mitochondrial oxidative stress triggers depolarization of mitochondrial membrane via oxidative modification of proteins.²⁸ Therefore, to prove the selective effects of MitoTBHP on mitochondria, we examined changes in MMP by fluorescence imaging using JC-1.²⁹ The JC-1 dye forms red fluorescent aggregates that accumulate in mitochondria at high potentials, whereas at low potentials, it exists as a monomer that emits green fluorescence. MCF-7 cells were preincubated with JC-1 (2 μM), followed by treatment with MitoTBHP (50 μM) for 15 min, irradiated with 375 nm (2.5 mW/cm²) light, and fluorescence imaging was performed 60 min later. The fluorescence of the JC-1 monomer was significantly higher in cells under light irradiation in the presence of MitoTBHP (Fig. 5a and S8a). In this case, the fluorescence intensity ratio of JC-1 monomer to JC-1 aggregate was twice that of the non-irradiated cells. In contrast, when the cells were treated with AcBhcTBHP, no significant changes in MMPs were observed with or without irradiation (Fig. 5b, S8b and S9). Similarly, light-irradiated cells in the presence of 50 μM TBHP did not show significant changes in MMPs, similar to light irradiation alone (Fig. S10). To induce MMP depolarisation, cells usually need to be treated with 100–500 μM H₂O₂ or TBHP^{7,9,29,30}, but MitoTBHP could induce significant changes in mitochondrial membrane potential upon photo-irradiation at only 5 μM (Fig. S11). These results indicate that MitoTBHP localises to the mitochondria and induces mitochondria-specific oxidative stress upon light irradiation.

In conclusion, we designed and synthesised a new caged hydroperoxide, BhcTBHP, consisting of a Bhc phototrigger and

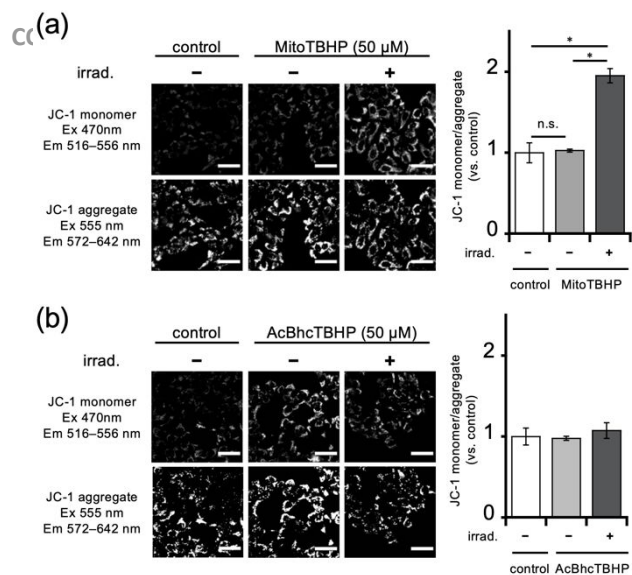


Fig. 5 Confocal fluorescence microscopic images of irradiated MCF-7 cells treated with (a) MitoTBHP or (b) AcBhcTBHP using JC-1. Scale bar = 50 μ m. The change of MMP of MCF-7 cells detected by the JC-1 ratio (JC-1 monomer/JC-1 aggregate fluorescence). The ratio of the control was defined with the control sample as 1.0. Average cellular fluorescence intensity of the MCF-7 cells was determined using Image J. Error bars denote standard error (SE; n=3). * p <0.001. Tukey's test.

TBHP as an effector, and successfully developed membrane-permeable AcBhcTBHP and mitochondria-targeted MitoTBHP. These caged compounds rapidly and efficiently released TBHP upon blue light irradiation. Furthermore, they also worked in an intracellular reducing environment, where light irradiation caused AcBhcTBHP to release TBHP into the cell and MitoTBHP induced MMP depolarisation by mitochondria-selective oxidative stress. Thus, the caged hydroperoxide can induce oxidative stress or redox signalling by generating pro-oxidants on demand in specific cell compartments. There is no precedent for such caged compounds that can control intracellular oxidative modifications in a spatiotemporal manner; in particular, MitoTBHP is expected to be useful for rigorous studies of redox signalling and oxidative stress. We are currently working to develop more stable and diverse organelle-targeted derivatives to elucidate intracellular and intercellular redox signalling.

This work was supported by JST, ACT-X (Grant Number JPMJAX1919 to M.T.), JSPS Grant-in-Aid for Scientific Research on Innovative Areas (19H05778 to H.N.) and the "Project on Opening Gifu's Future with Diverse Researchers". This work was inspired by the international environment of the JSPS Core-to-Core Program, "Asian Chemical Biology Initiative."

Conflicts of interest

There are not conflicts to declare.

Notes and references

- 1 S. A. Sinenko, T. Yu. Starkova, A. A. Kuzmin and A. N. Tomilin, *Front. Cell Dev. Biol.*, 2021, **9**, 714370.
- 2 C. Lennicke and H. M. Cochemé, *Mol. Cell*, 2021, **81**, 3691–3707.

- 3 M. Schieber and N. S. Chandel, *Curr. Biol.*, 2014, **24**, R453–R462.
- 4 N. Kaludercic, S. Deshwal and F. D. Lisa, *Front. Physiol.*, 2014, **5**, 285.
- 5 C. Martín, R. Martínez, R. Navarro, J. I. Ruiz-Sanz, M. Lacort and M. B. Ruiz-Larrea, *Biochem. Pharmacol.*, 2001, **62**, 705–712.
- 6 M. Marchetti, L. Resnick, E. Gamliel, S. Kesaraju, H. Weissbach and D. Binnering, *PLoS One*, 2009, **4**, e5804.
- 7 O. Kučera, R. Endlicher, T. Roušar, H. Lotková, T. Garnol, Z. Drahotka and Z. Červinková, *Oxid. Med. Cell Longev.*, 2014, **2014**, 752506.
- 8 W. Park, *Oncol. Rep.*, 2018, **40**, 1787–1794.
- 9 W. Zhao, H. Feng, W. Sun, K. Liu, J.-J. Lu and X. Chen, *Redox Biol.*, 2017, **11**, 524–534.
- 10 L. Wu, A. C. Sedgwick, X. Sun, S. D. Bull, X.-P. He and T. D. James, *Acc. Chem. Res.*, 2019, **52**, 2582–2597.
- 11 M. S. Messina, G. Quargnali and C. J. Chang, *ACS Bio. Med. Chem. Au.*, 2022, **2**, 548–564.
- 12 H. Nakagawa, *Chem. Pharm. Bull.*, 2016, **64**, 1249–1255.
- 13 T. C. Pham, V.-N. Nguyen, Y. Choi, S. Lee and J. Yoon, *Chem. Rev.*, 2021, **121**, 13454–13619.
- 14 E. W. Miller, N. Taulet, C. S. Onak, E. J. New, J. K. Lanselle, G. S. Smelick and C. J. Chang, *J. Am. Chem. Soc.*, 2010, **132**, 17071–17073.
- 15 T. Furuta, S. S.-H. Wang, J. L. Dantzker, T. M. Dore, W. J. Bybee, E. M. Callaway, W. Denk and R. Y. Tsien, *Proc. Natl. Acad. Sci. U. S. A.*, 1999, **96**, 1193–1200.
- 16 T. Furuta, *J. Synth. Org. Chem. Jpn.*, 2012, **70**, 1164–1169.
- 17 I. Cazin, E. Rossegger, G. G. de la Cruz, T. Griesser and S. Schlögl, *Polymers*, 2021, **13**, 56.
- 18 L. Josa-Culleré and A. Llebaria, *ChemPhotoChem*, 2021, **5**, 296–314.
- 19 B. Schade, V. Hagen, R. Schmidt, R. Herbrich, E. Krause, T. Eckardt and J. Bendig, *J. Org. Chem.*, 1999, **64**, 9109–9117.
- 20 P. Klán, T. Šolomek, C. G. Bochet, A. Blanc, R. Givens, M. Rubina, V. Popik, A. Kostikov and J. Wirz, *Chem. Rev.*, 2013, **113**, 199–191.
- 21 A. Z. Suzuki, T. Watanabe, M. Kawamoto, K. Nishiyama, H. Yamashita, M. Ishii, M. Iwamura and T. Furuta, *Org. Lett.*, 2003, **5**, 4867–4870.
- 22 K. Katayama, S. Tsukiji, T. Furuta and T. Nagamune, *Chem. Commun.*, 2008, 5399–5401.
- 23 S. Chalmers, S. T. Caldwell, C. Quin, T. A. Prime, A. M. James, A. G. Cairns, M. P. Murphy, J. G. McCarron and R. C. Hartley, *J. Am. Chem. Soc.*, 2012, **134**, 758–761.
- 24 M. Abo, Y. Urano, K. Hanaoka, T. Terai, T. Komatsu and T. Nagano, *J. Am. Chem. Soc.*, 2011, **133**, 10629–10637.
- 25 N. Senda, A. Momotake, Y. Nishimura and T. Arai, *Bull. Chem. Soc. Jpn.*, 2006, **79**, 1753–1757.
- 26 M. S. Baptista, J. Cadet, P. D. Mascio, A. A. Ghogare, A. Greer, M. R. Hamblin, C. Lorente, S. C. Nunez, M. S. Ribeiro, A. H. Thomas, M. Vignoni and T. M. Yoshimura, *Photochem. Photobiol.*, 2017, **93**, 912–919.
- 27 J. F. King, G. T. Y. Tsang, M. M. Abdel-Malik and N. C. Payne, *J. Am. Chem. Soc.*, 1985, **107**, 3224–3232.
- 28 C. Lee, J. S. Nam, C. G. Lee, M. Park, C.-M. Yoo, H.-W. Rhee, J. K. Seo and T.-H. Kwon, *Nat. Commun.*, 2021, **12**, 26.
- 29 F. Rizvi, A. Mathur, S. Krishna, M. I. Siddiqi and P. Kakkar, *Redox Biol.*, 2015, **6**, 587–598.
- 30 X. Xin, T. Gong and Y. Hong, *Sci. Rep.*, 2022, **12**, 14519.